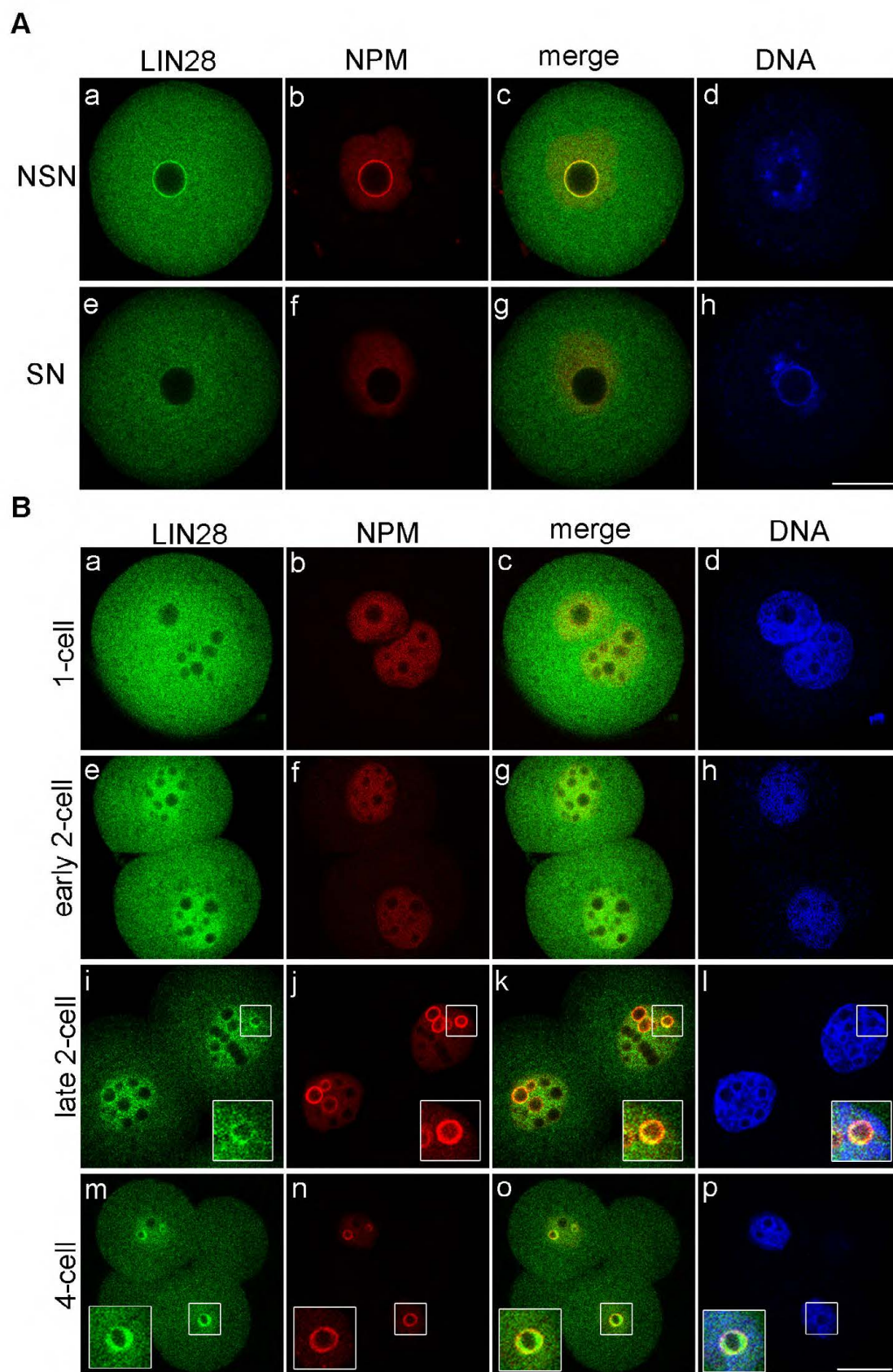
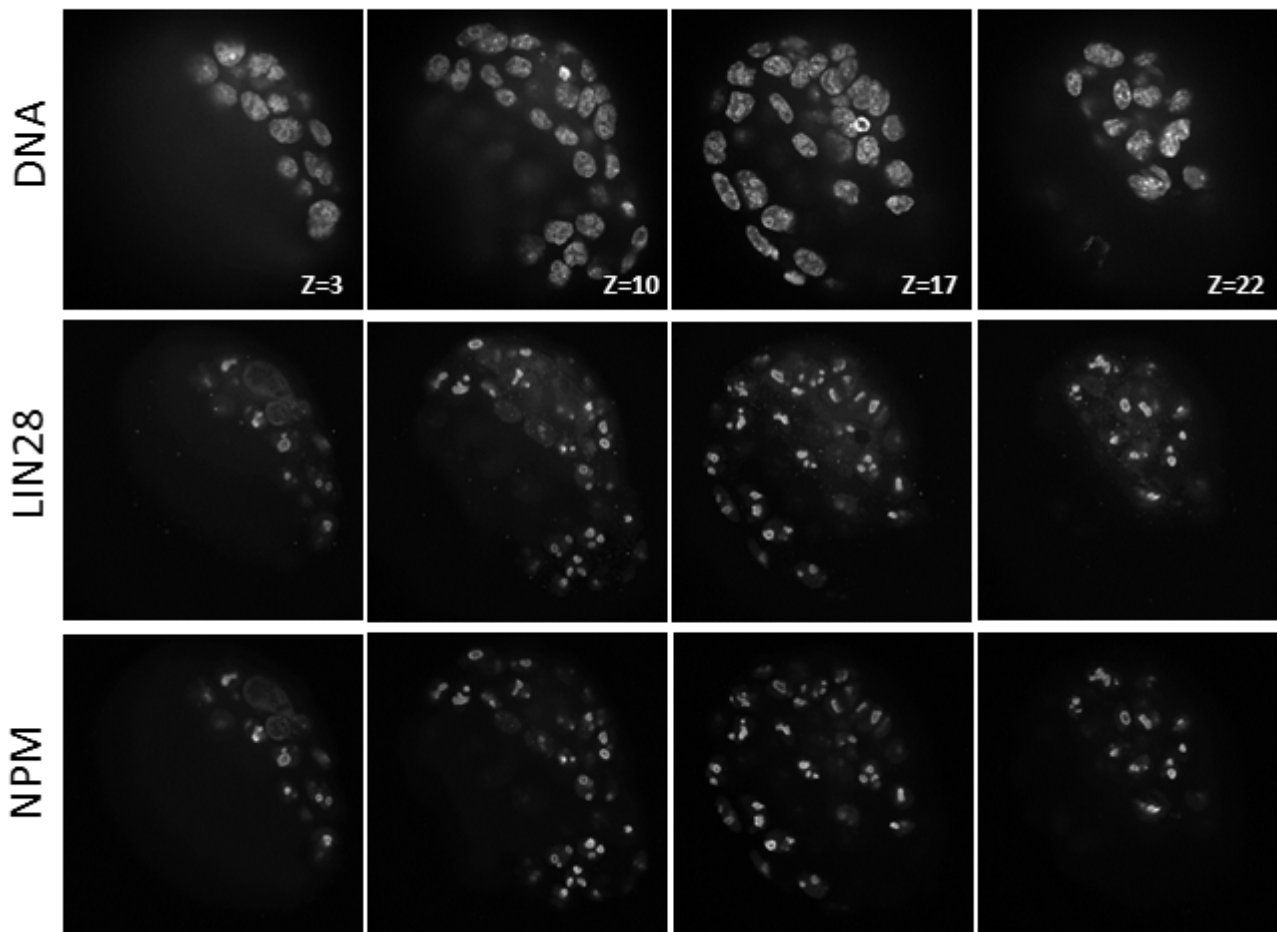


**Fig. S1. Cellular localization of LIN28 protein in mouse 2-cell embryos and mouse ESCs.** Confocal immunofluorescence analysis of endogenous LIN28 in whole-mount embryos. B23 (NPM) was used as a nucleolar marker. DNA was counterstained with DAPI. **(Aa-d)** LIN28 expression is absent in mid 2-cell embryos where no NPBs have been assembled. NPM is restricted to the nucleoplasm and not enriched at the periphery of presumptive NPBs. **(Ae-h)** Late 2-cell embryo showing one blastomere at the G2 stage, while the second blastomere is at M-phase. LIN28 colocalizes with B23/NPM at the periphery of a NPB (arrow) in the G2-staged blastomere. **(Ba-d)** Immunostaining of a mouse ESC line expressing GFP fused with histone H2B shows that LIN28 and B23/NPM colocalize in nucleoli (arrow). Scale bars: 20  $\mu$ m.



**Fig. S2. Cellular localization of LIN28 protein in fully-grown mouse F1 (C57BL/6xCBA/Tar) oocytes and during early preimplantation development of F1×F1 embryos.** Confocal immunofluorescence analysis of endogenous LIN28 in whole-mount oocytes and embryos. B23 (NPM) was used as a nucleolar marker. DNA was counterstained with DRAQ. **(A)** In NSN oocytes (Aa-d) LIN28 and NPM localize at the periphery of the nucleolus. During transition from NSN to SN configuration, both LIN28 and NPM gradually disappear from surface of the nucleolus and they are not detected there in SN oocytes (Ae-h). **(B)** In zygotes (Ba-d) and early 2-cell embryos (Be-h) homogenous nuclear signals of both LIN28 and NPM were observed. No enrichment at the periphery of nucleolar precursor bodies (NPBs) was observed. At late 2-cell stage (Bi-l) both LIN28 and NPM were observed at the periphery of NPBs, where they colocalized. This pattern was also observed in 4-cell embryos for both LIN28 and NPM (Bm-p). In these embryos, LIN28 fluorescent signal around NPBs was stronger than in late 2-cell embryos. Scale bars: 20  $\mu$ m.

## Mouse Blastocyst



**Fig. S3. Cellular localization of LIN28 protein in mouse blastocysts.** Confocal immunofluorescence analysis of endogenous LIN28 in whole-mount embryos. B23 (NPM) was used as a nucleolar marker. DNA was counterstained with DAPI. Different *z*-sections of the full projection (Fig. 2U-X) show that LIN28 is present both TE and ICM cells.

## Marmoset Morula

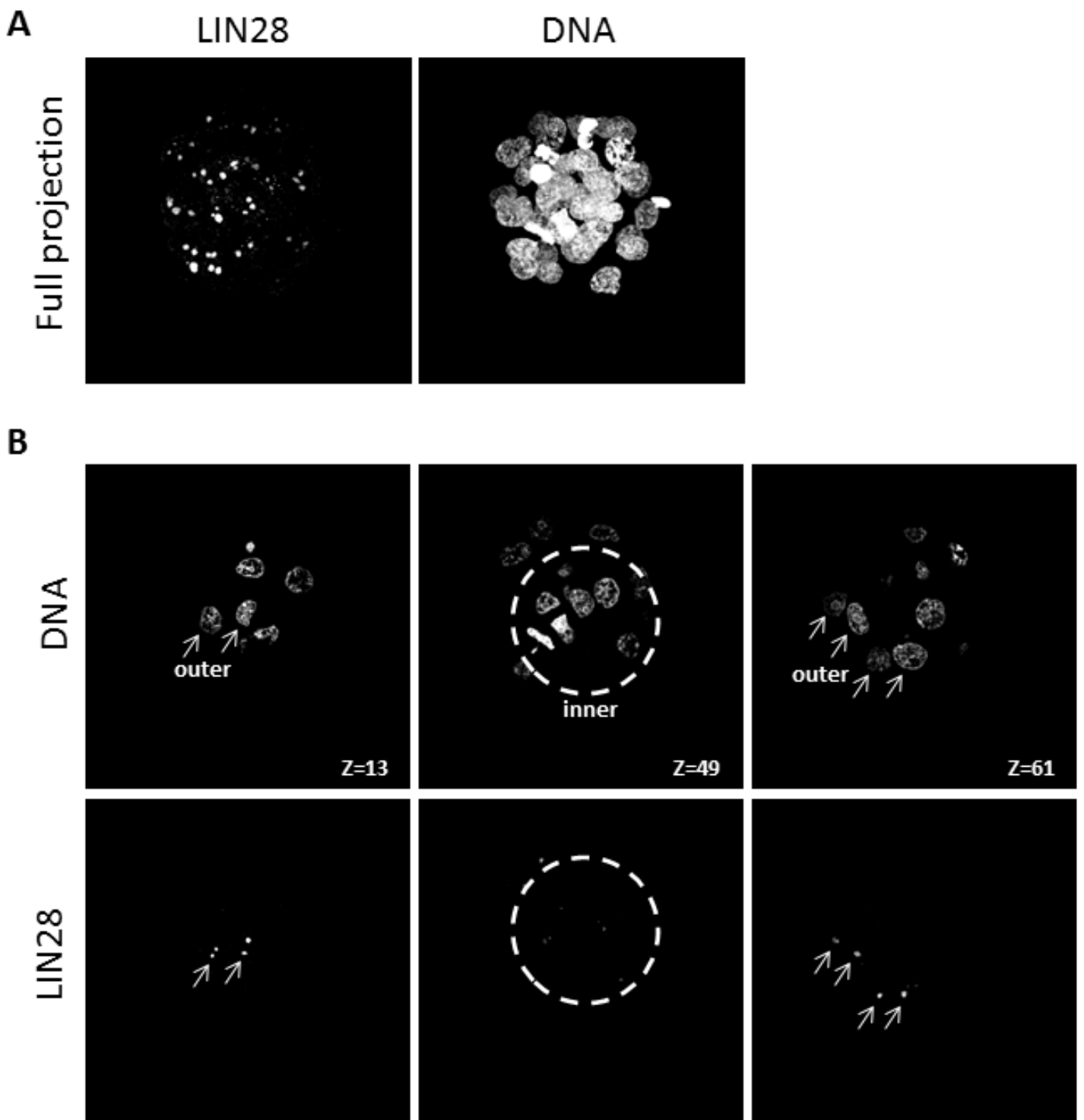


**Fig. S4. Cellular localization of LIN28 protein in morula-staged embryo of the common marmoset monkey.** Confocal immunofluorescence analysis of endogenous LIN28. DNA was counterstained with propidium iodide. **(A)** Full projection of a marmoset morula showing LIN28 and nuclei. **(B)** Different *z*-sections of the full projection show that LIN28 is present in nuclei of outer blastomeres (arrows), but absent in nuclei of inner blastomeres (dashed line).

## Marmoset Blastocyst

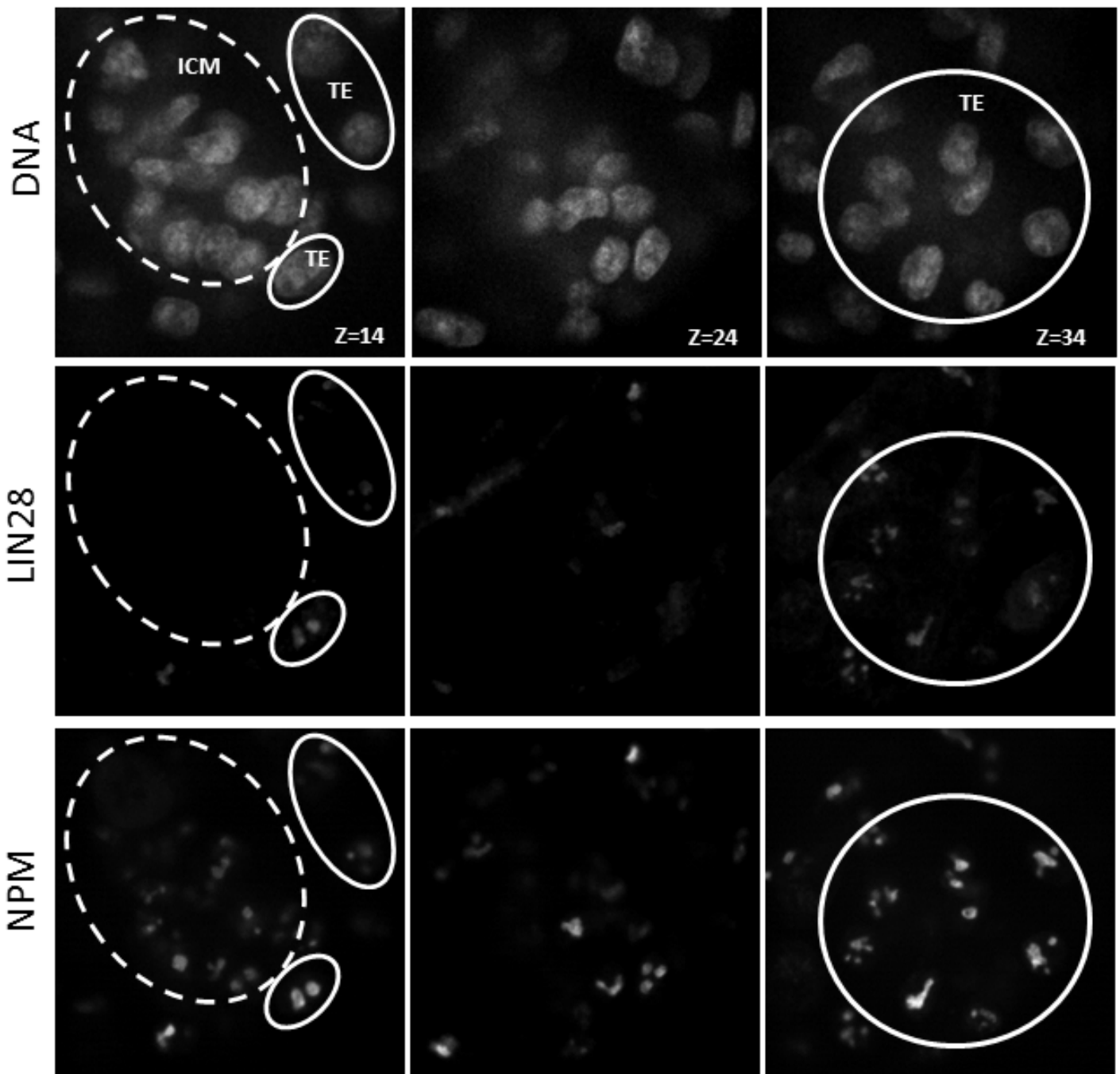


**Fig. S5. Cellular localization of LIN28 protein in blastocyst embryo of the common marmoset monkey.** Confocal immunofluorescence analysis of endogenous LIN28. B23 (NPM) was used as a nucleolar marker. DNA was counterstained with DAPI. Different z-sections of the boxed region (Fig. 5H) show that LIN28 is present in trophoblast cells (unbroken line), but absent in ICM cells (dashed line).